Digital Twin of Retail Environment Using RFID Particle Filter Localization

Christopher Turner[†], Dheeraj Bhaskaruni[‡], Xiangyu Wang[‡], Jian Zhang[§], Shiwen Mao,[†]
Senthilkumar CG Periaswamy,[‡] and Justin Patton[‡]
[†]Dept. Electrical & Computer Engineering, Auburn University, Auburn, AL 36845-5201, USA
[‡]RFID Lab, Auburn University, Auburn, AL 36830, USA
[§]Department of Information Technology, Kennesaw State University, Marietta, GA 30144, USA
Email: {cmt0106, dzb0098, xzw0042}@auburn.edu, {jianzhang, smao}@ieee.org, {szc0089, jbp0033}@auburn.edu,

***Abstract*—Localization using the RFID technology provides an effective solution for improving inventory accuracy in varying industries. The retail environment being an ever-growing topic of interest, our focus is on exploring Bayesian statistical algorithms centered on particle filter localization. With the use of stereo tracking cameras, we create a 3D point cloud of the environment in real time and localize a variety of items. This method is built upon a previous work that does not rely on RSSI or phase measurements. After the environment is transferred to a Digital Twin using RGB-D cameras, we can identify the position of various tags. To determine the performance of the proposed particle filter, we use a commercial off-the-shelf (COTS) storage rack to emulate a retail environment. A testing procedure is conducted to compare the proposed particle filter approach with the previous Bayesian filter approach. The proposed scheme performs adequately in heavy-clutter environments with a reduced computational time.**

***Index Terms*—Digital twin, Radio-frequency identification (RFID), Bayesian filter, Localization, Particle filter, Real-time appearance-based mapping (RTAB-Map)**

I. Introduction

The need for cost-effective inventory management systems at the commercial level has motivated innovative problem-solving techniques [1], [2]. With the rapid development of the Internet of Things (IoT), the *radio-frequency dentification* (RFID) technology has been widely adopted in many fields [3]–[5] for a broad range of applications such as retailing, asset tracking, healthcare, and supply chain management [6]. Radio frequency (RF) and ultra-wide band-width (UWB) hybrid real-time locating systems (RTLS) localization has became a worthwhile investment as industries search for future high-precision alternatives [7]. In the last two decades, RFID has become a popular choice for item localization due to these cost savings and simplicity of deployment [8]. The use of handheld RFID scanners has become a popular solution for retailers performing cycle counts regularly in their stores due to a lower cost of implementation.

The concept of *digital twin* has gained popularity with RFID researchers considering its utility for many fields, from improving customer services in the retail industry [9], [10] construction workplace safety [11], to cislunar operations [12]. A digital twin refers to a virtual representation (usually in the digital world) of a physical system, while the digital twinning technology aims at building a high-fidelity virtual model or depiction of a real-world entity or system, which involves both digital and physical elements [13]. With the integration of the RFID technology and digital twin, we can create precise models that better predict inventory status in an accurate and timely matter. Such an overview of the retail store will enable effective exploration and management of the retail store.

With the rapid growth since 2016, the digital twin has been considered a critical component of many fields. The innovative data streaming through digital twins could potentially benefit the real-world process [12], [14], [15]. This is shown in recent efforts to repair the industrial production of the modern world with an idea known as industry 4.0 (4IR). Using smart hardware, technologies, data collection, and IoT to improve the production pipeline, many researchers have recognized the digital twin technology as the next push for industrial innovation [16]. Simulation models can be transformed to establish a digital twin to interact with incoming data and optimize the model efficiency. For example, Braglia et al. [17] present an agent-based simulation model of a large paper warehouse, in which the forklifts and the pallets are identified by reading their attached Ultra High Frequency (UHF) RFID tags. The sensors update data for the locations of products and forklifts in the digital twin at certain time intervals. The simulation model (i.e., the digital twin) develops new alternative scenarios, attempting to optimize warehouse efficiency involving routes that forklifts traverse to minimize the overall costs of warehouse management. Then, the optimized routes are studied by staff and are then carefully followed.

The combination of robotics and digital twin technologies has been developed in the retail store and warehouse management scenarios. Various studies have focused on deploying RFID techniques to localize items to benefit inventory tracking [18]. The prior works mainly adopted RFID tags as landmarks to accurately pinpoint the tagged products [19]. Maïzi and Bendavid developed an RFID-based digital twin system for inventory tracking, customer monitoring, and operations management [9]. Smart-store designs leveraging ground robots to deploy inventory updates have shown improvements on customer experiences and store operations. This was also achieved by introducing machine learning to analyze the incoming data to enhance inventory accuracy [20].

In this paper, we present a pilot model of a retail store digital

twin based on the Real-Time Appearance-Based Mapping (RTAB-map) technology [21], where each product attached with an RFID tag is localized and marked in the digital twin model. Our system implements two RGB-D cameras to capture visual information and a handheld RFID reader to scan RFID tags. While the human operator is scanning RFID tags, both visual and localization data are fed into the digital twin model. The 3D digital twin is then constructed in real-time, and all scanned tags are labeled in the 3D environment of the generated retail store digital twin. The core of the proposed system is a classical Bayesian filtering method for passive UHF RFID tag localization. We prototype the system with commercial off-the-shelf (COTS) equipment in a single, representative retail scenario. The quantitative experimental results are examined to measure the accuracy of item-level tag localization. The experiments illustrated accurate localization results, which is within 0.367 m, achieved with multi-path effects present in the environment. Our particle filter-based localization scheme exhibits a computational speed improvement of roughly 2.5 times over that of the Bayesian filter. With the integration of digital twin and RFID localization in such retail store environments, our proposed system can greatly improve the efficiency of inventory and supply chain.

The rest of this paper is organized as follows. In Section II, we present the system design. In Section III, we present the experiment results. Section IV concludes this paper.

II. Methodology and Design

In this section, the Particle filter is first presented along with background on classical Bayesian filtering methods for passive UHF RFID tag localization. Then, we introduce the fixed transmit power RF model for improved location estimation. Finally, we describe the RTAB-Map method and demonstrate how the digital twin is established to merge the map and localization results, including coordinate transformation from camera frames to global frames.

A. Particle filter-based RFID localization

To begin, Bayesian filtering is known as a classical method that can be used to estimate the position of RFID tags. It is a probabilistic technique to estimate the state of a dynamic system (i.e., belief) over time by incorporating new observations while accounting for uncertainty. A detailed explanation can be found in our previous work [10]. Particle filtering implements a similar mathematical approach in which each particle represents a state of the overall system (i.e., position and orientation) denoted by the state space model:

$$x_k = f(x_{k-1}) + u_k \tag{1}$$

$$y_k = h(x_k) + n_k, \tag{2}$$

where x_k and y_k represent the systems internal state location and the measurements at each time step k, respectively; f is a non-linear state transition model function, while h is the measurement function; u_k and n_k represent an independent identically distributed (i.i.d.) process and the measurement noise sequence, respectively. This i.i.d. process directly correlates to any noise the system experiences and for our application, noise refers to inaccuracies due to the reader's movements.

The particle filter method utilizes the creation of a discrete approximation to the probability density function (pdf) found by the fundamental Bayesian state filtering problem. The pdfs of both u_k and n_k define the prior particle density $p(x_k|x_{k-1})$ and likelihood functions $p(y_k|x_k)$, respectively. Therefore, with $x_k^i, i = 1, 2, ..., N_s$ representing our particles and $w_k^i, i = 1, 2, ..., N_s$ the associated weights, we have the following particle update formula and weight update formula, respectively:

$$x_k^i \sim p(x_k|x_{k-1}^i) \tag{3}$$

$$w_k^i \propto w_{k-1}^i p(y_k|x_k^i). \tag{4}$$

Both equations are summarized as the sampling and weighting step respectively for all particle i, when $1 \leq i \leq N$. After the observed weights update from inferring the measurement model (2), we need to identify which particles consist of higher weights. A resampling step is required to discard particles with low weights and duplicate those with high weights. Many options for resampling exist, and we settled on a systematic resampling technique simplified to:

$$p(x_k|y_{1:k}) \approx \sum_{i=1}^{N_s} w_k^i \delta(x_k - x_k^i), \tag{5}$$

where $\delta(x_k - x_k^i)$ is a delta function centered at x_k^i.

Our resampling choice does not require sorting; instead, it selects new particles using a cumulative sum sweeping through each particle, which is linear in complexity. This is how we achieve a shorter computational time when referring to a Bayesian filter-based localization approach. This process can be summarized by dividing into five parts: (i) initialize with normal distribution assuming equal weights within the model, (ii) predict the next state of particles, (iii) update weights based on new measurement values, (iv) resample by discarding improbable particles, and (v) finally compute the RFID tag's estimated position:

$$x_{est} = \frac{\sum_{i=1}^{N} x_i w_i}{\sum_{i=1}^{N} w_i}. \tag{6}$$

Each estimated position x_{est} is derived from the weighted average of all particle position x_i. Rather than resampling at every step, we resample only when necessary, based on the effective sample size N_{eff}. This approach ensures that resampling occurs only when it can enhance the particle distribution. By leveraging N_{eff}, we can estimate the number of particles that meaningfully contribute to the probability distribution function (PDF), thereby maintaining diversity while minimizing unnecessary computations.

$$N_{eff} = \frac{1}{\sum w_i^2}. \tag{7}$$

This technique encompasses a broad selection of Monte Carlo algorithms for approximating the probability density of any distribution. Thrun [22] details the success of global localization in ground robots using Markov chain particle filtering, where this implementation consistently outperforms traditional techniques. In our test environment, it is assumed that the environment is static, which means that all the RFID tags are stationary and located in the detecting area during the experiments. As discussed, the user will hold the RFID reader with two cameras mounted to collect data at various positions. Every read of RFID tag response is recorded and correlated to the specific pose in the predetermined global map. Then, after all the readings from the RFID tags are received, the locations will be estimated using the Particle filter.

A two-dimensional (2D) illustration of the Particle filter is shown in Fig. 1, and the detailed steps are presented in Algorithm 1. At the beginning of the algorithm, all observed tags at their respective time k are assigned weights denoted by the weighting step $w_k^i \propto w_{k-1}^i p(y_k|x_k^i)$ only after all particles are normalized. The results of all estimated tags are dependent on the Bayes model $p(y_k|x_k^i)$. Then, as the weights get assessed, depending on their values, they will either resample or stay assigned to their respective particle. Finally, the estimated tag position is returned once all particles have been resampled. Testing performed in a complex experimental environment prevents simple modeling techniques from performing adequately. Therefore, numerous observations during each experiment are required. In other words, all observations captured by an RFID reader are used to examine the dynamic locations and orientations of all RFID tags. This become the basis for an applied empirical model created specifically to prevent poor performance in such environments. This model requires capturing all observations by an RFID reader at fixed positions, while the RFID tags are put at dynamic locations with random orientations.

The search area is evenly divided into a grid at a fixed spatial interval of 10 cm, and a tag is attached at the center of each grid during each recording. In each round of data collection, the reader's transmit power is constant. By putting an RFID tag in each grid, we can observe multiple reads from the reader. The observation collection process consists of 20 rounds of experiment, and we establish a map of successful readings from each grid in the area. The probabilistic RFID observation model is acquired, in which a higher observation probability indicates a larger number of successful readings. More details on the observation experiment can be found in our previous work [18]. The Particle filter with a fixed transmit power is developed based on the approaches in [23].

Algorithm 1 Particle filter for RFID tag localization

Input: RFID tag data, reader power level, and reader pose ;
Output: Estimated tag location after meaningful resampling steps have occurred ;

```
//N represents the total number of particles over the state space
for each time step k do
    Normalize particle weights so that their sum is equal to one ;
    for i = 1 to N do
        Compute an estimate of the state (estimated tag's position) as the weighted average of all particle states ;
        w_k^i ∝ w_{k-1}^i p(y_k|x_k^i) ;
    end forqwerp0;-
    for each scanned tag do
        Assessing particle weight concentration and determine effective number of contributing particles ;
        if N_eff < N/2 then
            Perform resample and assign updated weights to generate a new set of particles for high probability regions;
        end if
    end for
end for
return The estimated tag position ;
```

B. RTAB-Map based digital twin construction

Real-Time Appearance-Based Mapping (RTAB-Map) [21] is a powerful open-source approach of Simultaneous Localization And Mapping (SLAM) [24]. It is widely used in robotics localization and mapping studies to provide real-time environment map construction based on sensors such as cameras and LiDAR.

In this work, we create a digital twin model of our test environment by deploying RTAB-Map with two cameras mounted on an portable RFID reader. Specifically, the RealSense D435 camera, which is capable of capturing both RGB and depth images (i.e., RGB-D), is adopted to populate the essential data required for constructing a 3D map [25]. The RealSense T265, as a specialized tracking camera, offers odometry data to enable the localization and mapping of the scanning system [26]. Before data acquisition begins, the two cameras should be calibrated. This procedure comprises the identification and adjustment of both intrinsic and extrinsic parameters of the cameras to establish a precise correspondence between pixel coordinates and the global coordinates [25]. Synchronization of the sensing process plays an essential role in ensuring the creation of an accurate digital twin by aligning the visual data from both cameras with continuous RF signals. The visual features, such as key points and descriptors, are extracted from the RGB-D images acquired with the D435 camera. The odometry data gathered from the T265 camera offers motion estimation that facilitate feature matching over consecutive frames and the identification of loop closures [24]. Loop closure detection is the crucial procedure of comparing the current visual data with previously acquired data. It enhances the digital twin's consistency and mitigates drift when the system refines the map and the agent's estimated pose within the map. The RTAB-Map method leverages graph optimization to maximize the consistency and accuracy of the map based on the designed graph structure of inter-frame agent pose and landmarks.

To integrate the odometry data and the RGB-D data from both cameras, a comprehensive 3D spatial map as a digital twin of the target region is created. However, the pose of the two cameras mounted together on the RFID reader is described in the T265's built-in frame coordinate [25]. In the

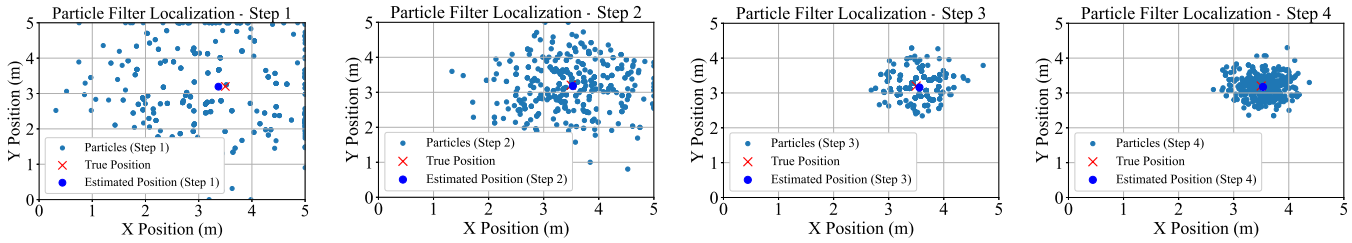

Fig. 1: An illustration of RFID tag localization with a Particle Filter. Over four steps (epochs), the weights are resampled to show the estimated tag location.

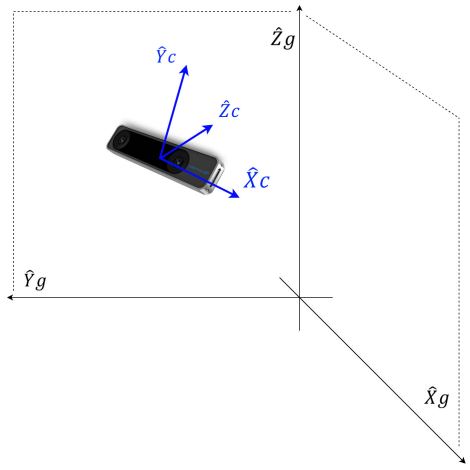

Fig. 2: The coordinate system: the global coordinate (g) and the camera local coordinate (c).

data acquisition phase, the user carries the RFID reader and camera system in the 3D space with six degrees of freedom (6-DoF) [19]. Its pose is defined as the combination of position **T** and orientation **R**, which are three translation DoFs and three rotation DoFs, respectively [27]. We assume a predetermined frame coordinates as $\mathcal{L}$ and a pose **P** is assigned to this coordinate according to its relative position and orientation of axes. A pose **P** related to coordinate frame $\mathcal{L}$ is given by:

$$\mathbf{P} = [\mathbf{T}, \mathbf{R}]^T, \tag{8}$$

where position **T** is a 3D vector, orientation **R** is a 3D matrix, and $(\cdot)^T$ denotes the transpose operation.

As illustrated in Fig. 2, we defined two coordinate systems to represent the camera-reader pose in the 3D space. One is the camera's local coordinates c, with an origin at the center point of the T265 camera. The other coordinate is the global coordinates g as the environment coordinate frame, with its origin located at a fixed location on the ground. The RFID reader detects a UHF tag at position $P_c = (x_c, y_c, z_c)^T$ in the local camera coordinate. To perform the rigid transformation from the camera coordinates to the global coordinates, the translation vector T_c^g and rotation matrix R_c^g are calculated. The 3D-translation represents the offset from the camera frame coordinates c relative to the global frame g, specified as:

$$T_c^g = [o_x^g - o_x^c, o_y^g - o_y^c, o_z^g - o_z^c]^T = [t_x, t_y, t_z]^T, \tag{9}$$

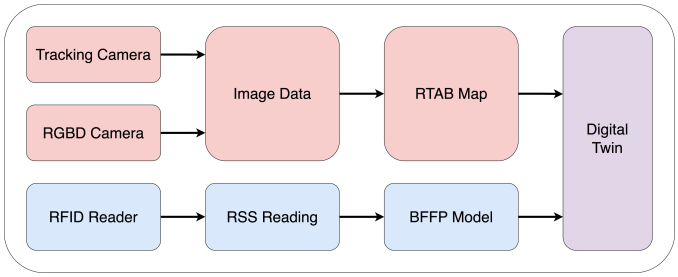

Fig. 3: System architecture of the proposed approach: blue colored blocks represent the RFID pipeline, whereas the peach colored blocks are for the visual components.

which $[o_x^c, o_y^c, o_z^c]$ and $[o_x^g, o_y^g, o_z^g]$ denote the origins of the camera coordinate frame and the global coordinate frame, respectively. The 3D-rotation matrix from the local camera coordinates to the global coordinates is specified as a 3×3 matrix, given by:

$$R_c^g = \begin{bmatrix} \hat{X}_c \cdot \hat{X}_g & \hat{Y}_c \cdot \hat{X}_g & \hat{Z}_c \cdot \hat{X}_g \\ \hat{X}_c \cdot \hat{Y}_g & \hat{Y}_c \cdot \hat{Y}_g & \hat{Z}_c \cdot \hat{Y}_g \\ \hat{X}_c \cdot \hat{Z}_g & \hat{Y}_c \cdot \hat{Z}_g & \hat{Z}_c \cdot \hat{Z}_g \end{bmatrix} = \begin{bmatrix} r_{11} & r_{12} & r_{13} \\ r_{21} & r_{22} & r_{23} \\ r_{31} & r_{32} & r_{33} \end{bmatrix},$$

where $\hat{X}_c$, $\hat{Y}_c$, and $\hat{Z}_c$ denote the unit vector of local camera coordinate axes and $\hat{X}_g$, $\hat{Y}_g$, $\hat{Z}_g$ denote the unit vector of global coordinate axes. Based on the derived translation vector T_c^g and rotation matrix R_c^g, the frame coordinate transformation from local camera to global is given by:

$$\begin{aligned} P_g &= R_c^g \cdot P_c + T_c^g \\ &= \begin{bmatrix} r_{11} & r_{12} & r_{13} \\ r_{21} & r_{22} & r_{23} \\ r_{31} & r_{32} & r_{33} \end{bmatrix} P_c + [t_x, t_y, t_z]^T, \end{aligned} \tag{10}$$

By exporting the transformed tag locations to the RTAB-Map built 3D real-time map, we establish the digital twin of the target area, which contains the visual features, structural geometry, and the RFID tags localization results. The system architecture of the proposed method is illustrated in Fig. 3.

III. Experiments and Results

A. Experimental setup

To evaluate the performance of the model, a series of experiments are conducted in the RFID Lab of Auburn University.

The experiment environment consists of a single shoe rack populated with 40 tags on its 5 shelves as shown in Fig. 4(a). This rack is 1.82 m x 1.00 m and is placed in a 106 m^2 sized room with the rack placed directly in the center.

As shown in Fig. 5, a Realsense D435 RGB-D camera and a Realsense T265 tracking camera are mounted on top of a Zebra RFD8500 Bluetooth Handheld UHF RFID Reader, creating a proposed RF-visual sensing prototype. The RGB-D camera and the tracking camera are connected to a mini-computer through USB3 Type-C and USB Micro B cables, respectively. Connection between the Zebra RFD8500 reader [28] and the host computer is established via Bluetooth 2.1.

ROS Noetic is executed on Ubuntu for synchronizing all sensors in the proposed prototype. The passive UHF RFID tags we use is the Avery Dennison AD-237 [29]. It has an IC-type Impinj Monza R6 and 96-bit EPC for identification. The system is capable of localizing any specific tag model and other types of tags have been recognized but are not evaluated during our testing. To evaluate the performance of the tag localization in the digital twin, we conduct a small-scale experiment. In this test, the shoe rack is scanned and its digital twin is created. The actual location of the tags attached to the shoes are measured to serve as the ground truth.

B. Experimental results and discussions

Fig. 4(b) shows an example of the digital twin we built for the shoe rack to evaluate the performance of the proposed prototype in a small-scale scenario. All the RFID tags are localized and shown in the figure as red dots. This digital twin is created by the proposed method performed with the equipment shown in Fig. 5. For data collection, a user carries the equipment along with a host mini-computer holstered across their body to explore the target area. RGB-D images and RFID tag readings are captured to build the real-time digital twin of the shoe rack. All the shelves are scanned in 360 degrees at various heights using a consistent vertical and horizontal motion with the reader an even distance of roughly 1 m from the rack. Each test is accomplished within 2 minutes. The small-scale scenario experiment is performed in a highly cluttered environment with multi-path effect present from other tags not associated with the rack during each test. Five testing repetitions are performed at a fixed reader level of 12dB with 1 minute time intervals between tests. The localization error is then combined and averaged across all tests.

From each test, our computation time is significantly lower than Bayesian-filter localization for localizing all 40 tags, as shown in Table I. All the tags are distributed within a reasonable range using this proposed particle filter method. The average localization error from all tests is 0.367 m and the maximum error is 0.392 m in this experiment.

(a) The shoe rack.

(b) The digital twin of the shoe rack.

Fig. 4: An example digital twin built for a shoe rack to evaluate the proposed system.

TABLE I: Mean Localization Time Comparison

Filter	Mean Localization Time Per Tag
Particle Filter	0.954 Seconds
Bayesian Filter	2.49 Seconds

IV. Conclusions

This work developed an alternative statistical model for portable localization of a digital twin retail environment, using data collected by two cameras and a portable RFID reader. A particle filter-based RFID tag localization algorithm was examined using the previous antenna model implementation for real-time spatial mapping. The proposed particle filter

Fig. 5: The RF-visual sensing component: Realsense D435 RGB-D camera (Top), Realsense T265 tracking camera (Middle), and the Zebra RFD8500 Bluetooth Handheld UHF RFID Reader (Bottom).

performed adequately in heavy-clutter environments with the presence of multi-path effect while reducing the computational time. Performance of the model's tag localization showed an average error across all tests of 0.367 m. Multi-model handheld digital twin inventory localization could achieve significant improvements for specialized use cases. Future models could be trained and adjusted to fit retailers needs for achieving higher efficiency in inventory management.

ACKNOWLEDGMENT

This work is supported in part by the NSF under Grants CCSS-2245608 and CCSS-2245607.

REFERENCES

[1] C. Saygin, "Adaptive inventory management using rfid data," *Int. J. Adv. Manuf. Technol.*, vol. 32, pp. 1045—1051, Jan. 2007.

[2] S. Alyahya, Q. Wang, and N. Bennett, "Application and integration of an RFID-enabled warehousing management system–A feasibility study," *Elsevier J. Ind. Inform. Integration*, vol. 4, pp. 15–25, Dec. 2016.

[3] J. Zhang, S. Mao, S. Periaswamy, and J. Patton, "Standards for passive UHF RFID," *ACM GetMobile*, vol. 23, no. 3, pp. 10–15, Sept. 2019.

[4] X. Wang, J. Zhang, Z. Yu, S. Mao, S. C. Periaswamy, and J. Patton, "On remote temperature sensing using commercial uhf rfid tags," *IEEE Internet of Things Journal*, vol. 6, no. 6, pp. 10 715–10 727, Sept. 2019.

[5] X. Wang, J. Zhang, S. Mao, S. Periaswamy, and J. Patton, "MulTLoc: RF hologram tensor filteing and upscaling for indoor localization using multiple UHF passive RFID tags," in *Proc. ICCCN 2021*, Athens, Greece, July 2021, pp. 1–9.

[6] E. Elbasani, P. Siriporn, and J. S. Choi, "A survey on RFID in Industry 4.0," in *Internet of Things for Industry 4.0*, G. Kanagachidambaresan, R. Anand, E. Balasubramanian, and V. Mahima, Eds. Cham, Switzerland: Springer, 2020, ch. 1, pp. 1–16.

[7] C. Zhai, Z. Zou, Q. Zhou, J. Mao, Q. Chen, H. Tenhunen, L. Zheng, and L. Xu, "A 2.4-Ghz ISM RF and UWB hybrid RFID real-time locating system for industrial enterprise Internet of Things," *Enterprise Information Systems*, vol. 11, no. 6, pp. 909–926, Mar. 2017.

[8] B. C. Hardgrave, J. A. Aloysius, and S. Goyal, "RFID-enabled visibility and retail inventory record inaccuracy: Experiments in the field," *Prod. Oper. Manag.*, vol. 22, no. 4, pp. 843–856, Mar. 2013.

[9] Y. Maizi and Y. Bendavid, "Building a digital twin for IoT smart stores: A case in retail and apparel industry," *Int. J. Simulation and Process Modelling*, vol. 16, no. 2, pp. 147–160, June 2021.

[10] J. Ma, X. Wang, C. Powell, J. Zhang, S. Mao, S. C. Periaswamy, and J. Patton, "Digital twin of retail stores with RFID tags localization," in *Proc. 9th International Conference on Smart and Sustainable Technologies (SpliTech)*, Split, Croatia, June 2024, pp. 01–06.

[11] S. P. Anikesh Paul and D. J. U. Maheswari, "Digital twin framework for worker safety using RFID technology," in *Proc. Int. Symp. Automation and Robotics in Construction*, Chennai, India, July 2023, pp. 254–261.

[12] F. Quazi, A. Vaequez-Castro, D. Niyato, S. Mao, and Z. Han, "Building delay-tolerant digital twins for cislunar operations using age of synchronization," in *Proc. IEEE ICC 2024 Workshops*, Denver, CO, June 2024.

[13] D. Jones, C. Snider, A. Nassehi, J. Yon, and B. Hicks, "Characterising the digital twin: A systematic literature review," *CIRP journal of manufacturing science and technology*, vol. 29, pp. 36–52, May 2020.

[14] F. Tao, H. Zhang, A. Liu, and A. Y. Nee, "Digital twin in industry: State-of-the-art," *IEEE Transactions on Industrial Informatics*, vol. 15, no. 4, pp. 2405–2415, Sept. 2018.

[15] G. Moiceanu and G. Paraschiv, "Digital twin and smart manufacturing in industries: A bibliometric analysis with a focus on Industry 4.0," *MDPI Sensors*, vol. 22, no. 4, p. 1388, Feb. 2022.

[16] V. Voipio, K. Elfvengren, J. Korpela, and J. Vilko, "Driving competitiveness with RFID-enabled digital twin: case study from a global manufacturing firm's supply chain," *Measuring Business Excellence*, vol. 27, no. 1, pp. 40–53, Jan. 2023.

[17] M. Braglia, R. Gabbrielli, M. Frosolini, L. Marrazzini, and L. Padellini, "Using RFID technology and discrete-events, agent-based simulation tools to build digital-twins of large warehouses," in *Proc. IEEE RFID-TA 2019*, Pisa, Italy, Sept. 2019, pp. 464–469.

[18] J. Zhang, Y. Lyu, J. Patton, S. C. Periaswamy, and T. Roppel, "BFVP: A probabilistic UHF RFID tag localization algorithm using Bayesian filter and a variable power RFID model," *IEEE Transactions on Industrial Electronics*, vol. 65, no. 10, pp. 8250–8259, Feb. 2018.

[19] J. Zhang, X. Wang, Z. Yu, Y. Lyu, S. Mao, S. C. Periaswamy, J. Patton, and X. Wang, "Robust RFID based 6-DoF localization for unmanned aerial vehicles," *IEEE Access*, vol. 7, pp. 77 348–77 361, June 2019.

[20] R. Pous, M. Chindemi, and A. Alajami, "Showing products in a retail store digital twin with item location captured by an RFID robot," in *Proc. IEEE RFID-TA 2023*, Aveiro, Portugal, Sept. 2023, pp. 189–192.

[21] M. Labbe and F. Michaud, "Appearance-based loop closure detection for online large-scale and long-term operation," *IEEE Transactions on Robotics*, vol. 29, no. 3, pp. 734–745, Feb. 2013.

[22] S. Thrun, "Particle filters in robotics." in *UAI*, vol. 2. Citeseer, 2002, pp. 511–518.

[23] I. Ehrenberg, C. Floerkemeier, and S. Sarma, "Inventory management with an RFID-equipped mobile robot," in *Proc. 2007 IEEE International Conference on Automation Science and Engineering*, Scottsdale, AZ, Oct. 2007, pp. 1020–1026.

[24] M. Labbé and F. Michaud, "RTAB-map as an open-source lidar and visual simultaneous localization and mapping library for large-scale and long-term online operation," *Journal of Field Robotics*, vol. 36, no. 2, pp. 416–446, Oct. 2019.

[25] L. Keselman, J. Iselin Woodfill, A. Grunnet-Jepsen, and A. Bhowmik, "Intel realsense stereoscopic depth cameras," in *Proc. IEEE CVPR 2017 Workshops*, Honolulu, HI, July 2017, pp. 1–10.

[26] P. Schmidt, J. Scaife, M. Harville, S. Liman, and A. Ahmed, "Intel® realsense™ tracking camera t265 and intel® realsense™ depth camera d435-tracking and depth," accessed: Mar. 2024. [Online]. Available: https://dev.intelrealsense.com/docs/depth-and-tracking-cameras-alignment

[27] J. Zhang, Z. Yu, X. Wang, Y. Lyu, S. Mao, S. C. Periaswamy, J. Patton, and X. Wang, "RFHUI: An RFID based human-unmanned aerial vehicle interaction system in an indoor environment," *KeAi Digital Communications and Networks*, vol. 6, no. 1, pp. 14–22, May 2020.

[28] Z. Technologies, "Zebra RFD8500 Handheld RFID," accessed: Mar. 2024. [Online]. Available: https://www.zebra.com/us/en/products/rfid/rfid-handhelds/rfd8500.html

[29] A. Dennison, "Avery Dennison Smartrac AD-237r6 UHF RFID," accessed: Mar. 2024. [Online]. Available: https://www.atlasrfidstore.com/avery-dennison-smartrac-ad-237r6-uhf-rfid-white-wet-inlay-monza-r6/